Published OnlineFirst August 1, 2007; DOI: 10.1158/1535-7163.MCT-07-0070

A novel, potent, and selective insulin-like growth factor-I receptor kinase inhibitor blocks insulin-like growth factor-I receptor signaling *in vitro* and inhibits insulin-like growth factor-I receptor–dependent tumor growth *in vivo*

Qun-sheng Ji, Mark J. Mulvihill, Maryland Rosenfeld-Franklin, Andrew Cooke, Lixin Feng, Gilda Mak, Matthew O'Connor, Yan Yao, Caroline Pirritt, Elizabeth Buck, Alexandra Eyzaguirre, Lee D. Arnold, Neil W. Gibson, and Jonathan A. Pachter

(OSI) Oncology, OSI Pharmaceuticals, Inc., New York, New York

Abstract

Insulin-like growth factor-I receptor (IGF-IR) and its ligands, IGF-I and IGF-II, are up-regulated in a variety of human cancers. In tumors, such as colorectal, non–small cell lung, ovarian, and pediatric cancers, which may drive their own growth and survival through autocrine IGF-II expression, the role of IGF-IR is especially critical. Here, we present a novel small-molecule IGF-IR kinase inhibitor, *cis*-3-[3-(4-methyl-piperazin-l-yl)-cyclobutyl]-1-(2-phenyl-quinolin-7-yl)-imidazo[1,5-*a*]pyrazin-8-ylamine (PQIP), which displayed a cellular IC_{50} of 19 nmol/L for inhibition of ligand-dependent autophosphorylation of human IGF-IR with 14-fold cellular selectivity relative to the human insulin receptor. PQIP showed minimal activity against a panel of 32 other protein kinases. It also abolished the ligand-induced activation of downstream phosphorylated AKT and phosphorylated extracellular signal-regulated kinase 1/2 in both IGF-IR transfectant cells and a GEO human colorectal cancer cell line. Analysis of GEO cells revealed a significant level of both phosphorylated IGF-IR and IGF-II expression. Furthermore, inactivation of IGF-II in conditioned GEO culture medium by a neutralizing antibody diminished IGF-IR activation, indicating the presence of a functional IGF-II/IGF-IR autocrine loop in GEO cells. Once daily oral dosing of PQIP induced robust antitumor efficacy in GEO xenografts. The antitumor efficacy correlated with the degree and duration of inhibition of tumor IGF-IR phosphorylation *in vivo* by this compound. Moreover, when mice were treated for 3 days with a dose of PQIP that maximally inhibited tumor growth, only minor changes in blood glucose were observed. Thus, PQIP represents a potent and selective IGF-IR kinase inhibitor that is especially efficacious in an IGF-II–driven human tumor model. [Mol Cancer Ther 2007;6(8):2158–67]

Introduction

The insulin-like growth factor-I receptor (IGF-IR) is a tetrameric transmembrane receptor tyrosine kinase that is widely expressed in normal human tissues and is involved in embryonic development and postnatal growth. The receptor is composed of two α and two β subunits linked by disulfide bonds. The extracellular α subunit is responsible for ligand binding, whereas the β subunit consists of a transmembrane domain and a cytoplasmic tyrosine kinase domain. The receptor is activated by its cognate ligands, insulin-like growth factor-I (IGF-I) and IGF-II, and to a lesser extent by insulin (500- to 1,000-fold less potent; ref. 1). Ligand binding activates the intrinsic tyrosine kinase activity of IGF-IR, resulting in trans-β subunit autophosphorylation and the stimulation of signaling cascades that include the IRS-l/phosphatidylinositol 3-kinase/AKT/mammalian target of rapamycin and growth factor receptor binding protein 2/Sos/Ras/mitogen-activated protein kinase pathways. Activation of IGF-IR has been reported to stimulate proliferation, survival, transformation, metastasis, and angiogenesis (1–6). Inhibition of IGF-IR by various approaches, including antisense (7, 8), anti–IGF-IR antibodies (9–12), dominant-negative IGF-IR (13–15), and small-molecule inhibitors (16–19), has been shown to reduce tumor growth in human tumor xenograft models. Increased expression of IGF-I and IGF-II and their corresponding receptor, IGF-IR, has been shown in a broad range of solid tumors and hematologic neoplasias relative to corresponding normal tissue (3–6, 20–23). IGF-I is mainly produced in the liver, whereas IGF-II is synthesized locally in an autocrine or paracrine manner. Because IGF-IIR is a monomeric binding protein without tyrosine kinase activity, IGF-IR seems to function as the predominant signaling receptor for both IGF-I and IGF-II. The link between cancer and IGF signaling is further supported by epidemiologic studies showing an increased relative risk for the development of colon, prostate, breast, lung, and bladder cancers in individuals with circulating IGF-I levels in the upper tertile of the reference range (24–28). Moreover, tumor IGF-IR expression correlates with poor prognosis in renal cell carcinoma (29). Furthermore, IGF-IR

Received 1/31/07; revised 5/2/07; accepted 6/29/07.

The costs of publication of this article were defrayed in part by the payment of page charges. This article must therefore be hereby marked *advertisement* in accordance with 18 U.S.C. Section 1734 solely to indicate this fact.

Requests for reprints: Qun-sheng Ji, Department of Cancer Biology, 1 Bioscience Park Drive, Farmingdale, NY 11735. Phone: 631-962-0670; Fax: 631-845-5671. E-mail: qji@osip.com

doi:10.1158/1535-7163.MCT-07-0070

Published OnlineFirst August 1, 2007; DOI: 10.1158/1535-7163.MCT-07-0070

signaling may be a mechanism of resistance to various antitumor therapies, including epidermal growth factor receptor inhibitors (30). It is notable that although no specific mutations in IGF receptors or ligands have been identified in cancers, there is clear evidence of epigenetic alterations; that is, loss of imprinting or other regulatory failures that lead to increased IGF-II expression in a variety of human tumors, including colorectal (31, 32), ovarian (33, 34), lung (35), liver (36), and pediatric cancers (23). Indeed, *IGF-II* is the gene most overexpressed in colon cancers compared with normal colonic mucosa (31) and loss of imprinting of *IGF-II* represents a risk factor for colorectal cancer (37). These data clearly indicate that an active IGF-II autocrine loop can play an important role in colon cancer progression.

Here, we report a potent and selective IGF-IR tyrosine kinase inhibitor, *cis*-3-[3-(4-methyl-piperazin-l-yl)-cyclobutyl]-1-(2-phenyl-quinolin-7-yl)-imidazo[1,5-*a*]pyrazin-8-ylamine (PQIP), that potently inhibits human IGF-IR with 14-fold selectivity over human insulin receptor (IR) in intact cells. Moreover, PQIP inhibits cell proliferation and induces apoptosis through a mechanism that includes inhibition of AKT activation. The promising pharmacokinetic and pharmacodynamic properties of the compound together with robust antitumor activity observed in an IGF-II autocrine xenograft model suggest potential clinical utilities for IGF-IR kinase inhibitors, such as PQIP, in colon cancer and other human malignancies.

Materials and Methods

Synthesis of PQIP

PQIP is a 1,3-disubstituted-8-amino-imidazopyrazine derivative (Fig. 1A) synthesized by the methods described in patent application WO 2005/097800 A1 (38). Compound identity and purity (>99%) were verified by ^{1}H and ^{13}C nuclear magnetic resonance, mass spectrometry, and high-performance liquid chromatography using Bruker Avance 400, WatersMicromass ZQ, and Waters LC Module I Plus instruments, respectively, as well as by elemental analysis. PQIP was dissolved in DMSO at 10 mmol/L for use in biochemical or cellular *in vitro* assays. For *in vivo* studies, PQIP was dissolved in 25 mmol/L tartaric acid at an appropriate concentration to deliver the desired dose of 10 mL/kg by oral gavage.

Cell Lines

3T3/huIGF1R fibrosarcoma cells, derived from NIH 3T3 cells stably overexpressing full-length human IGF-IR, were obtained from Dr. J. Beebe (Pfizer, Inc., Ann Arbor, MI). GEO human colorectal cancer cells were kindly provided by Dr. M. Brattain (Roswell Park Cancer Institute, Buffalo, NY) and were maintained in McCoy's 5A medium supplemented with 10% FCS and 1% L-glutamine or in serum-free conditioned culture system. Cell lines NCI-H292, HepG2, Hepa-1, SW620, Colo205, SW480, HT29, HCT116, HCT8, MCF-7, DU4475, BxPC3, MiaPaca2, HPAC, Panc1, and A1165 were grown in medium as prescribed by the American Type Culture Collection containing 10% FCS.

Antibodies

The following antibodies were used for immunoprecipitation or as the capture antibody in ELISA assays: human IGF-IR (Ab-1, Calbiochem), human IR (Lab Vision Corp.), and mouse IR (Santa Cruz Biotechnology) for capture; human IGF-IRβ (Santa Cruz Biotechnology) for immunoprecipitation. The following antibodies were used for immunoblotting analysis: human IGF-IRβ (Santa Cruz Biotechnology), antiphosphotyrosine (Exalpha Biologicals), antiphosphotyrosine-horseradish peroxidase (HRP) conjugate (mouse anti-phosphotyrosine-HRP, Invitrogen-Zymed), phosphorylated AKT^{T308} (Cell Signaling Technology), phosphorylated AKT^{S473} (Cell Signaling Technology), total AKT (Cell Signaling Technology), phosphorylated extracellular signal-regulated kinase 1/2 (ERK1/2; Cell Signaling Technology), total ERK1/2 (Cell Signaling Technology), p-p70S6K (Cell Signaling Technology), and cleaved poly(ADP)ribose polymerase (Cell Signaling Technology).

Animals

Female CD-1 and athymic nude *nu/nu* CD-1 mice (6–8 weeks, 25–29 g) were obtained from Charles River Laboratories. Animals were allowed to acclimate for a minimum of 1 week before initiation of a study. Throughout the studies, animals were allowed sterile rodent chow and water *ad libitum*, and immunocompromised animals were maintained under specific pathogen-free conditions. All animal studies were conducted at OSI facilities with the approval of the Institutional Animal Care and Use Committee in an American Association for Accreditation of Laboratory Animal Care–accredited vivarium and in accordance with the Institute of Laboratory Animal Research (Guide for the Care and Use of Laboratory Animals, NIH, Bethesda, MD).

Protein Kinase Biochemical Assays

Protein kinase assays were either done in-house by ELISA-based assay methods (IGF-IR, IR, Kit, epidermal growth factor receptor, and kinase insert domain receptor) or at Upstate, Inc., by a radiometric method (KinaseProfiler service). In-house ELISA assays used poly(Glu:Tyr) (Sigma) as the substrate bound to the surface of 96-well assay plates, and phosphorylation was detected using an anti-phosphotyrosine antibody conjugated to HRP. The bound antibody was quantified using 2,2′-azino-bis(3-ethylbenzthiazoline-6-sulfonic acid) as the peroxidase substrate by measuring absorbance at 405/490 nm. All assays used purified recombinant kinase catalytic domains. Recombinant enzymes of human IGF-IR, Kit, or epidermal growth factor receptor were expressed as an NH_2-terminal glutathione *S*-transferase fusion protein in insect cells, and were purified in-house (39). The human IR protein was purchased from Calbiochem.

Protein Kinase Inhibition in Intact Cells

Quantitative 96-well ELISA assays were developed to study the cellular effects of PQIP. Cells were plated into 96-well plates and cultured overnight before serum starvation (0.5% FCS) at 37°C for 2 h (3T3/huIGF1R) or overnight (HepG2 and Hepa-1). They were then treated

Published OnlineFirst August 1, 2007; DOI: 10.1158/1535-7163.MCT-07-0070

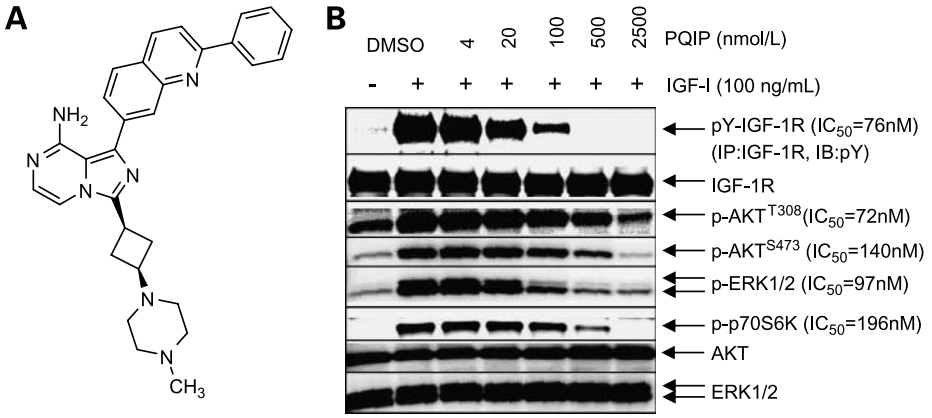

Figure 1. Inhibition of ligand-stimulated phosphorylated IGF-IR, phosphorylated AKT, phosphorylated ERK1/2, and phosphorylated p70S6K by PQIP in 3T3/huIGF1R cells. **A,** chemical structure of PQIP. **B,** serum-starved 3T3/huIGF1R cells were incubated with PQIP at indicated concentrations for 2 h at 37°C, followed by stimulation with IGF-I ligand for 15 min. Cell lysates were then analyzed by immunoprecipitation and immunoblotting for both total and phosphorylated (*p*-) target protein content. IC_{50} values were calculated based on the phosphorylated protein content quantified using densitometry.

with various concentrations of compound for 2 h before lysis (the final DMSO concentration in the assay was 0.4%), and IGF-I (100 ng/mL, R&D Systems) or insulin (10 ng/mL, Roche) was added for the final 15 min of the compound treatment period. Lysates were prepared in TGH buffer [1% Triton X-100, 10% glycerol, 50 mmol/L HEPES (pH 7.4); ref. 40] supplemented with 150 mmol/L NaCl, 1.5 mmol/L MgCl, 1 mmol/L EDTA, and fresh protease and phosphatase inhibitors (10 μg/mL leupeptin, 25 μg/mL aprotinin, and 200 μmol/L Na_3VO_4). ELISA assays of the target protein phosphorylation were done by transferring lysates into a second 96-well plate that was precoated with the appropriate capture antibody. The target proteins were then probed with an antiphosphotyrosine antibody HRP conjugate using a chemiluminescent HRP substrate (Pierce) for detection by luminometry. In experiments to evaluate the effect of plasma protein binding on PQIP potency, whole plasma from mouse, dog, or human was incorporated into the quantitative 96-well assays at a concentration of 90%. In these experiments, plasma was added to the cell culture medium before compound addition.

For immunoblotting analysis, lysates were cleared of insoluble material by centrifugation at 15,000 × *g* for 5 min at 4°C and the resultant supernatant was subjected to immunoprecipitation with the appropriate antibody coupled to Protein G-Sepharose beads (Sigma), followed by SDS-PAGE and immunoblotting with antiphosphotyrosine antibody-HRP conjugate and chemiluminescent detection. Alternatively, for highly abundant protein targets [IGF-IR, ERK1/2, AKT, p70S6K and cleaved-poly(ADP)ribose polymerase], lysates were analyzed directly by SDS-PAGE and immunoblotting.

Cell Proliferation and Anchorage-Independent Growth

For assays of cell proliferation, cells were seeded into 96-well plates and incubated for 3 days in the presence of PQIP at various concentrations. Inhibition of cell growth was determined by luminescent quantitation of intracellular ATP content using CellTiterGlo (Promega).

For assay of anchorage-independent growth, 2× MEM (phenol-red free, Invitrogen-Life Technologies) supplemented with 20% FCS and 2% L-glu were mixed in a 1:1 ratio with 1.4% Nobel agar (BD Bioscience) to prepare a bottom layer (0.7% final agar) in six-well plates. After solidification of the bottom layer, GEO cell suspensions were plated in semisolid medium containing 0.35% agar MED, 10% FCS, and compound at indicated concentrations. The plates were incubated at 37°C for 14 to 18 days. Colonies were scored with the alpha imager (Alpha Innotech) after 2 h staining with methylthiazolyldiphenyltetrazolium bromide (1 mg/mL).

IGF-II Autocrine IGF-IR Phosphorylation in GEO Cells

For analysis of an IGF autocrine loop in intact cells, cells were seeded into 10-mm dishes in the appropriate cell culture medium supplemented with 10% FCS. After 24 h, the cell culture medium was replaced with fresh medium without FCS for the indicated time periods. Cells were then stimulated with or without IGF-I (100 ng/mL, R&D Systems) for 15 min before being lysed, followed by immunoanalysis of phosphorylated IGF-IR content. To prepare conditioned medium, media were collected from 72 h incubation of GEO or NCI-H292 cultures in the appropriate medium containing 0.1% bovine serum albumin without FCS, and then centrifuged at 15,000 × *g* for 10 min at 4°C to remove all contaminating cells. The conditioned medium was then preincubated with either normal IgG or an IGF-II neutralizing antibody (AF-292-NA, R&D Systems) for 2 h at 37°C before stimulating serum-starved NCI-H292 cells for 15 min at 37°C. The cells were lysed and proteins were analyzed by immunoprecipitation and immunoblotting for total and phosphorylated IGF-IR, phosphorylated AKT, or phosphorylated ERK1/2 as described above.

For detecting mRNA for IGF-I or IGF-II, ~5 × 10^6 cells were collected and RNA was isolated using a Perfect RNA mini kit (Eppendorf). Five micrograms of RNA were treated with DNase (New turbo DNA-free, Ambian) in a volume of 12.5 μL. A 5 μL aliquot of the DNase-treated RNA was used for cDNA synthesis using Super Script first-strand kit (Invitrogen), according to the manufacturer's instructions. PCR reaction mixes consisted of 2.5 μL of cDNA, 200 nmol/L each of 5′ and 3′ primers and 0.625 units of Taq DNA polymerase gold (PE Applied Biosystems) in 25 μL of PCR buffer A (2.5 mmol/L $MgCl_2$, and 200 μmol/L

Published OnlineFirst August 1, 2007; DOI: 10.1158/1535-7163.MCT-07-0070

deoxynucleotide triphosphates). For amplification of IGF-I, 35 cycles of PCR reactions were programmed as follows: 94°C, 1 min/55°C, 1 min/72°C, 2 min, followed by a final 5-min extension at 72°C. For PCR of IGF-II, the annealing temperature was raised to 60°C. The primers for amplification of IGF-I were as follows: *IGF-I* sense, 5′-CTCTCAACATCTCCCATCTC-3′; *IGF-I* antisense, 5′-CCTCCTTAGATCACAGCTCC-3′. The primers for amplification of *IGF-II* sequences were *IGF-II* sense, 5′-AGTCGATGCTGGTGCTTCTCA-3′ and *IGF-II* antisense 5′-GTGGGCGGGGTCTTGGGTGGGTAG-3′.

Pharmacokinetic Analysis of PQIP

For pharmacokinetic analysis, the compound was formulated in saline adjusted to pH 2 with 0.01 mol/L hydrochloric acid for i.v. injection, and in 25 mmol/L tartaric acid for oral administration. Female CD-1 mice (6–10 weeks old) received either a single i.v. dose (10 mg/kg) or a single oral dose (5–200 mg/kg) of compound. For i.v. dosing, compound was delivered via tail vein injection at a dosing volume of 4 mL/kg. For oral dosing, compound was delivered via oral gavage in a dosing volume of 10 mL/kg. Subsequently, three animals were sacrificed at each designated time point and blood samples were collected in EDTA. After centrifugation at 1,500 × *g* for 10 min, plasma samples were prepared by protein precipitation with methanol and analyzed by high-performance liquid chromatography-tandem mass spectrometry (PE Sciex API 3000 LC/tandem mass spectrometry System, Applied Biosystems). Pharmacokinetic variables for the plasma time-concentration profile, including C_{max}, area under the curve (AUC), elimination half-life ($t_{1/2}$), volume of distribution at steady-state (V_{ss}), clearance, mean residence time, and oral bioavailability, were calculated by noncompartmental analysis.

Pharmacodynamic Analysis of Phosphorylated IGF-IR Inhibition *In vivo*

To assess the ability of compounds to inhibit phosphorylated IGF-IR in tumors, female *nu/nu* CD-1 mice were implanted s.c. with either 3T3/huIGF1R or GEO cells. When tumors reached ~300 mm^3, mice were orally dosed with vehicle or compound, at the indicated doses. Both tumors and plasma were collected at appropriate time points for analysis of IGF-IR phosphorylation (tumor samples) and PQIP concentrations (plasma samples). The phosphorylation status of IGF-IR was determined by the following: Tumors were homogenized in 1 mL TGH buffer per 200 mg tumor using a tissue homogenizer (TissueTearor, BioSpec) on ice at 5,000 to 30,000 rpm until the tumor tissue was completely broken down. Following preclearing by centrifugation at 14,000 rpm for 5 min at 4°C, ~1 mg of tumor lysate was incubated with an antiphosphotyrosine antibody overnight at 4°C with rotation, and 30 μL Protein-A Sepharose (Sigma) was then added and incubation continued for an additional 2 h to overnight at 4°C. The immunoprecipitates were separated on SDS-PAGE and immunoblotted with a total IGF-IR antibody (Santa Cruz) followed by detection using an HRP-conjugated goat anti-rabbit IgG antibody (Cell Signaling) with enhanced chemiluminescence. For determination of total IGF-IR, a direct immunoblotting was used as described above using the sc-713 antibody. The phosphorylated IGF-IR and total IGF-IR bands were quantified using a Bio-Rad GS-800 Densitometer. The phosphorylated IGF-IR signal was normalized to total IGF-IR.

In vivo Antitumor Efficacy

Cells were harvested from cell culture flasks during exponential cell growth, washed twice with sterile PBS, counted, and resuspended in PBS to a suitable concentration before s.c. implantation on the right flank of *nu/nu* CD-1 mice. Tumors were established to 200 ± 50 mm^3 in size before randomization into treatment groups of eight mice each for efficacy studies. PQIP or vehicle was administered orally as indicated. Body weights were determined twice weekly along with tumor volume {V = [length × (width)^2] / 2} measurements using Vernier calipers during the study. Tumor growth inhibition (TGI) was determined at different time points by the following formula: % TGI = $(1 - \{(T_t / T_0) / (C_t / C_0)\} / 1 - \{C_0 / C_t\}) \times 100$, where T_t = median tumor volume of treated at time t, T_0 = median tumor volume of treated at time 0, C_t = median tumor volume of control at time t, and C_0 = median tumor volume of control at time 0. Mean TGI was calculated for the entire dosing period, with 50% TGI considered to be the minimal response required for efficacy. Growth delay was calculated as $T - C$, where T and C are the times in days for median tumor size in the treated (T) and control (C) groups to reach 400% of the initial tumor volume. Cures were excluded from this calculation.

Glucose Tolerance Test

CD-1 mice were dosed orally for 3 consecutive days with PQIP or vehicle. Mice were fasted for 8 h (water *ad libitum*) before final administration of treatments. Glucose (D-dextrose in water for injection, 20% solution) was administered at 2 g/kg by i.p. injection immediately after the third oral dose of compound (41). Blood samples were collected for glucose evaluation by tail vein stick at various time points after final compound dosing. Blood glucose levels were measured using a Glucose-201 instrument from HemoCue, Inc.

Results and Discussion

In vitro Activity of PQIP in Biochemical Assays

PQIP (Fig. 1A) was designed and subsequently optimized through structure-based design efforts that built upon cocrystal structures of earlier benzyloxyphenyl-derived imidazopyrazines with IGF-IR and IR (data not shown). PQIP potently inhibits the activity of recombinant kinase domains derived from the closely related receptor tyrosine kinases IGF-IR and IR when assayed using poly(Glu:Tyr) as the substrate at an ATP concentration of 100 μmol/L (Supplementary Table S1).[1] Both a cocrystal

[1] Supplementary material for this article is available at Molecular Cancer Therapeutics Online (http://mct.aacrjournals.org/).

Published OnlineFirst August 1, 2007; DOI: 10.1158/1535-7163.MCT-07-0070

Table 1. Inhibition of proliferation and colony formation of 3T3/huIGF1R and GEO cells by PQIP

Cell	3T3/hulGF1R cells			GEO cells		
Assay	Proliferation			Proliferation		Soft agar
Conditions	0.5% FCS + IGF-I	0.5% FCS + IGF-II	10% FCS	0.5% FCS	10% FCS	10% FCS
IC_{50} (μmol/L)	0.02	0.03	4.15	0.81	0.60	0.08

NOTE: Effect of PQIP on 3T3/huIGF1R and GEO cell proliferation was assessed using CellTiterGlo luciferase-based cellular ATP assay kit. Cells were seeded into 96-well plates under indicated conditions and incubated for 3 d in the presence of PQIP at various concentrations. Cell growth was determined by measuring intracellular ATP content. Effect of PQIP on anchorage-independent growth of GEO cells was determined using colony formation in soft agar assay in normal growth medium (containing 10% FCS) after 14- to 18-d treatment with PQIP.

structure and kinetic observations of effects of ATP on potency indicate that PQIP binds competitively to the ATP-binding pocket (data not shown). PQIP has also been assayed for inhibitory activity against 32 additional purified protein kinases representing tyrosine and serine/threonine kinase families and <50% inhibitory activity for these kinases was observed at 10 μmol/L of PQIP (Supplementary Table S1). ATP at 100 μmol/L concentration was used in the kinase profiling for direct comparison with IGF-IR and IR kinase activities. Hence, the counter-screening data indicate that PQIP is a potent and selective IGF-IR kinase inhibitor versus the kinases that were profiled, and the only known activity of significance is the inhibition of the highly homologous insulin receptor.

In vitro Activity of PQIP in Intact Cells

PQIP was tested for inhibition of ligand-stimulated IGF-IR tyrosine kinase activity in intact cells. In 3T3/huIGF1R cells, an NIH-3T3 line stably overexpressing full-length human IGF-IR, PQIP fully inhibits IGF-I–stimulated receptor tyrosine autophosphorylation using immunoprecipitation and immunoblotting analysis of cell lysates (Fig. 1B). PQIP also inhibits IGF-I–stimulated AKT and ERK1/2 signaling pathways in 3T3/huIGF1R cells. In addition to phosphorylated IGF-IR, phosphorylated ERK, and phosphorylated AKT inhibition, similar dose-dependent reduction in the level of phosphorylated p70S6K was observed when the cells were exposed *in vitro* to PQIP (Fig. 1B). In cell-based functional assays, PQIP inhibited IGF-I– and IGF-II–induced proliferation of 3T3/huIGF1R cells, and showed reduced antiproliferative potency in the presence of 10% FCS, suggesting that other serum factors can drive proliferation of this cell line through receptors other than IGF-IR (Table 1).

To functionally assess the influence of plasma protein binding on the biological potency of the compound across various species, 90% whole plasma from mouse, dog, or human was included in the IGF-IR cellular autophosphorylation assay. Significantly different shifts in the cellular potency of PQIP were observed upon the inclusion of plasma from several species (Table 2). The greatest potency shift was observed in the presence of mouse plasma, which increased the IC_{50} by ~45-fold, whereas lesser effects were observed with human and dog plasma (~6- to 7-fold IC_{50} increases). These differential potency shifts of PQIP were consistent with direct measurements of the binding of PQIP to plasma proteins from these species conducted at Ricerca Biosciences (data not shown), suggesting that greater exposures will be necessary in mice than in dogs and humans to overcome the effects of plasma. Because 90% whole plasma was used in the assay to predict physiologically relevant plasma exposures, the differential protein binding effects may be used to estimate equivalent exposures in other species relative to the efficacy observed in mouse models when assessing the therapeutic window of PQIP.

IGF-IR/IR Selectivity of PQIP in Intact Cells

To assess the ability of PQIP to inhibit the human IR tyrosine kinase in intact cells, a cellular assay using a human hepatoma cell line (HepG2) was developed. The IC_{50} of PQIP for human IR was 261 nmol/L in HepG2 cells (Table 2). HepG2 cells predominantly express IR (both A and B isoforms) and minimal IGF-IR, and insulin does not appreciably activate IGF-IR at the concentrations used in the assay (e.g., 10 ng/mL; data not shown; ref. 42). Hence, PQIP was found to be ~14-fold more potent toward human IGF-IR than human IR (Table 2). It was also found that mouse IR is more sensitive to PQIP than human IR

Table 2. Activity and selectivity of PQIP in intact cells

Target	IGF-IR				Insulin receptor	
Species	Human				Human	Mouse
+ 90% plasma	None	Human	Dog	Mouse	None	None
IC_{50} (μmol/L)	0.019	0.111	0.135	0.853	0.261	0.090
Selectivity (IR/IGF-IR)					14-fold	4-fold

NOTE: IC_{50} for inhibition of ligand-stimulated targets in intact cells was determined using a quantitative ELISA assay. For human IGF-IR, 3T3/huIGF1R cells were serum starved for 2 h and then treated with PQIP for 2 h in the absence or presence of 90% whole plasma from either human, dog, or mouse, followed by stimulation with IGF-I ligand (100 ng/mL) for 15 min. For human IR (HepG2) or mouse IR (Hepa-1), the cells were starved overnight before 2-h treatment with PQIP, followed by 15-min stimulation with human insulin (10 ng/mL). Inhibition of the target enzymes was determined by monitoring effects of IGF-I or insulin-stimulated receptor autophosphorylation. IC_{50} values were determined from the sigmoidal dose-response plot of percentage inhibition versus $\log_{10}$ compound concentration (Xlfit 3.0, IDBS). Fold selectivity for human IGF-IR relative to human or mouse IR was calculated by dividing the IC_{50} values for IR by the IC_{50} values for human IGF-IR.

Published OnlineFirst August 1, 2007; DOI: 10.1158/1535-7163.MCT-07-0070

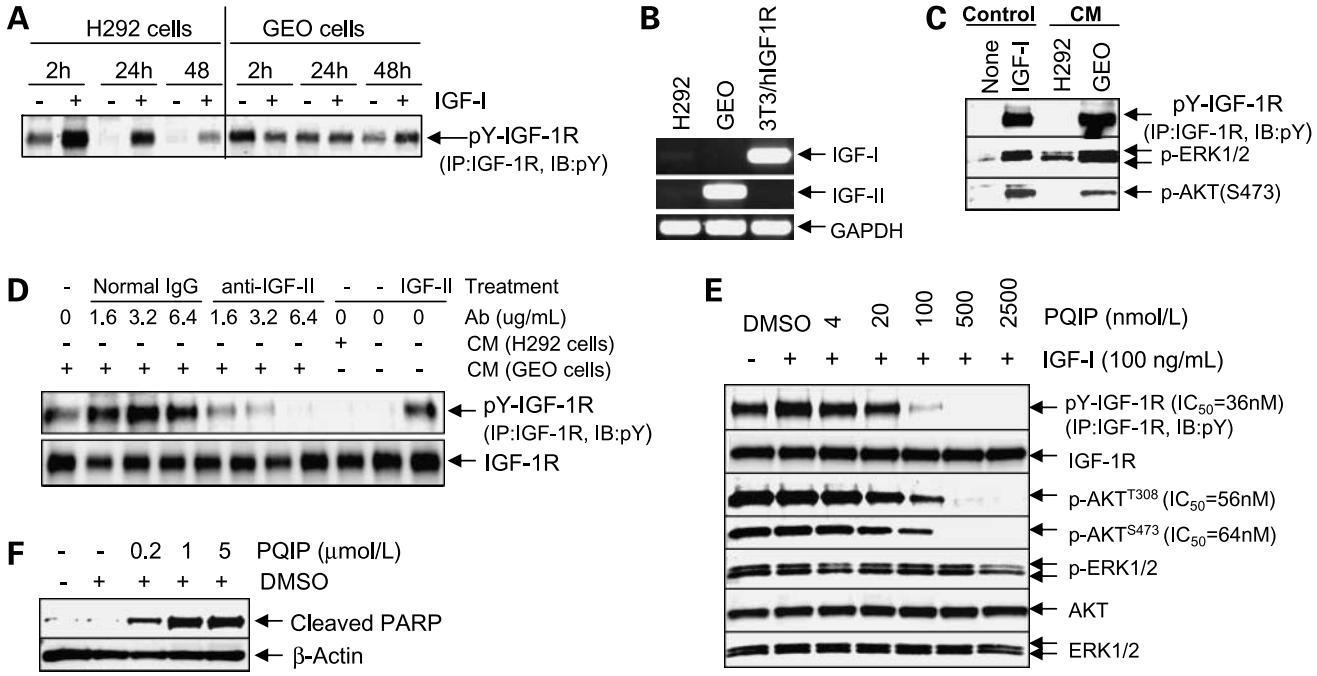

Figure 2. Active IGF-II/IGF-IR autocrine loop in GEO cells and inhibition of the autocrine activation of IGF-IR by PQIP. **A,** NCI-H292 and GEO cells were cultured in serum-free DMEM medium for indicated times, and then stimulated with or without IGF-I (100 ng/mL) for 15 min. Cell lysates were analyzed using immunoprecipitation (*IP*) and immunoblotting (*IB*) for both total and phosphorylated target protein content. **B,** mRNA expression of IGF-I or IGF-II was detected using reverse transcription-PCR in NCI-H292, GEO, and 3T3/huIGF1R cells. **C,** phosphorylated IGF-IR, AKT, and ERK1/2 were assessed by immunoprecipitation and immunoblotting in serum-starved NCI-H292 cells stimulated with GEO or NCI-H292 conditioned medium (*CM*). **D,** phosphorylated IGF-IR was assessed in serum-starved NCI-H292 cells stimulated with GEO conditioned culture medium that was preincubated with a neutralizing IGF-II antibody or nonspecific IgG at indicated concentrations. **E,** GEO cells cultured in normal growth medium (containing 10% FCS) were treated with PQIP at indicated concentrations for 2 h at 37°C with or without IGF-I (100 ng/mL) stimulation. Cell lysates were then analyzed by immunoprecipitation and immunoblotting for both total and phosphorylated target protein content. IC_{50} values were calculated based on the phosphorylated protein content quantified using densitometry. **F,** poly(ADP)ribose polymerase (*PARP*) cleavage in GEO cells after 24-h treatment with PQIP at indicated concentrations in the presence of 10% FCS, assessed by immunoblotting.

when assayed using a mouse hepatoma cell line Hepa-1 (Table 2), which expresses mouse IR but lacks IGF-IR (data not shown). The IGF-IR/IR selectivity of PQIP was further confirmed by determination of IGF-IR IC_{50} values in additional cell lines expressing endogenous human IGF-IR (HT29 and A431) and determination of IR IC_{50} values in primary human hepatocytes that express only IR. These cell lines showed comparable IGF-IR and IR potencies to those determined with 3T3/huIGF1R and HepG2 cells (data not shown). The selectivity for IGF-IR over IR is observed in the intact cell system, but not in the *in vitro* biochemical assays where the recombinant protein fragments corresponding to IGF-IR or IR are used, suggesting that conformation and selectivity may differ from the native enzymes in intact cells. IGF-IR/IR selectivity in cells, but not with *in vitro* enzymatic assays, has previously been reported (16). These data suggest that cellular assays may be preferred over biochemical assays to meaningfully assess selectivity of a novel pharmacologic agent between closely related target enzymes (39).

Blockade of the Active IGF-II/IGF-IR Autocrine Loop by PQIP in a Human GEO Colorectal Cancer Cell Line

To assess the effects of PQIP beyond the artificial 3T3/huIGF1R cell line, GEO human colorectal cancer cells were further evaluated for both basal phosphorylation of IGF-IR and expression of IGF-I and IGF-II (Fig. 2). Compared with the NCI-H292 non–small cell lung carcinoma cell line, the GEO cell line has significant and sustained basal phosphorylation of IGF-IR for at least 48 h under serum-free conditions without ligand stimulation (Fig. 2A). Accordingly, mRNA for IGF-II but not for IGF-I was detected in GEO cells, whereas little to no IGF-I or IGF-II mRNA was detected in NCI-H292 cells (Fig. 2B). In addition, conditioned medium derived from GEO cells stimulated tyrosine phosphorylation of IGF-IR in serum-starved NCI-H292 cells (Fig. 2C). The effect of conditioned medium on IGF-IR phosphorylation was diminished in a dose-dependent manner when the conditioned medium was preincubated with a neutralizing anti–IGF-II antibody (ref. 43; Fig. 2D). These data clearly suggest the presence of an active IGF-II/IGF-IR autocrine loop in GEO cells.

The ability of PQIP to block the IGF-II/IGF-IR autocrine loop in GEO cells was further evaluated through measurement of effects on downstream signaling pathways. PQIP blocks the active IGF-II autocrine loop in GEO cells as indicated by the complete inhibition of IGF-I–stimulated phosphorylation of IGF-IR well below the basal phosphorylation level. Furthermore, PQIP effectively inhibited AKT

Published OnlineFirst August 1, 2007; DOI: 10.1158/1535-7163.MCT-07-0070

activation but not ERK1/2 activation in the presence of 10% FCS (Fig. 2E), suggesting that phosphorylated AKT is IGF-IR dependent and ERK1/2 can be activated by non–IGF-IR–dependent mechanisms in GEO cells (Fig. 2E). Accordingly, PQIP was found to effectively induce apoptosis in GEO cells in the presence of 10% FCS, as indicated by induction of poly(ADP)ribose polymerase cleavage (Fig. 2F; ref. 44) and induction of DNA fragmentation (data not shown). In cell-based functional assays, the antiproliferative potency of PQIP is comparable between 0.5% FCS and 10% FCS (Table 1), suggesting that autocrine IGF-II is the main driver for GEO cell proliferation even in the presence of serum. Furthermore, GEO cells show increased sensitivity to PQIP when grown in soft agar (Table 1), consistent with the role of IGF-IR in cell transformation (1–3). These data clearly show that PQIP effectively blocks the active IGF-II/IGF-IR autocrine loop essential for GEO cell growth and survival. Moreover, the effect of PQIP on inhibition of cell proliferation was directly compared with two neutralizing antibodies against IGF-IR, MAB391 and α-IR3, in an MCF-7 human breast cancer cell line (45). PQIP was found to have similar activity when compared with the antibodies (Supplementary Fig. S1). Taken together, these results, along with the kinase selectivity data, indicate that the biological effects of PQIP are a direct result of blockade of IGF signaling.

Effect of PQIP on Tumor Cell Proliferation

The effect of PQIP on tumor cell proliferation was determined among a panel of human tumor cell lines (Supplementary Table S2). A number of colorectal, breast, and pancreatic cancer cell lines responded, indicating that IGF-IR kinase inhibitors may show broad antitumor activity regardless of tumor type. All of these cell lines were found to express IGF-IR (not shown), although there was no direct correlation between IGF-IR expression level and sensitivity to PQIP. The reasons for insensitivity of some cell lines are unclear, but could relate to expression of ABC transporters (known for Panc1), activating mutations in downstream signaling components (e.g., phosphatidylinositol 3-kinase mutation in HCT116) or dependence on growth factor receptors other than IGF-IR.

It was noted that the IC_{50} (600 nmol/L) for inhibition of proliferation (Table 1) is higher than that (36 nmol/L) for inhibition of phosphorylated IGF-IR (Fig. 2E) in GEO cells. Although the possibility of an off-target activity of PQIP against kinase(s) not measured cannot be ruled out, one more likely explanation for the observed difference in the IC_{50} values may be that GEO cells can also respond to autocrine IGF-II with an IR-A–mediated proliferative response. IR-A, an insulin receptor splice variant lacking exon 11, is known to function as a high-affinity receptor for IGF-II and mediates predominantly proliferative effects compared with the principally metabolic effects elicited by insulin stimulation of the IR-B isoform that includes exon 11 (1). GEO cells were found to express mRNA for IR-A at a level ~10-fold less than IGF-IR as determined by reverse transcription-PCR (data not shown). Because IGF-II may also stimulate proliferation of GEO cells via IR-A, and PQIP

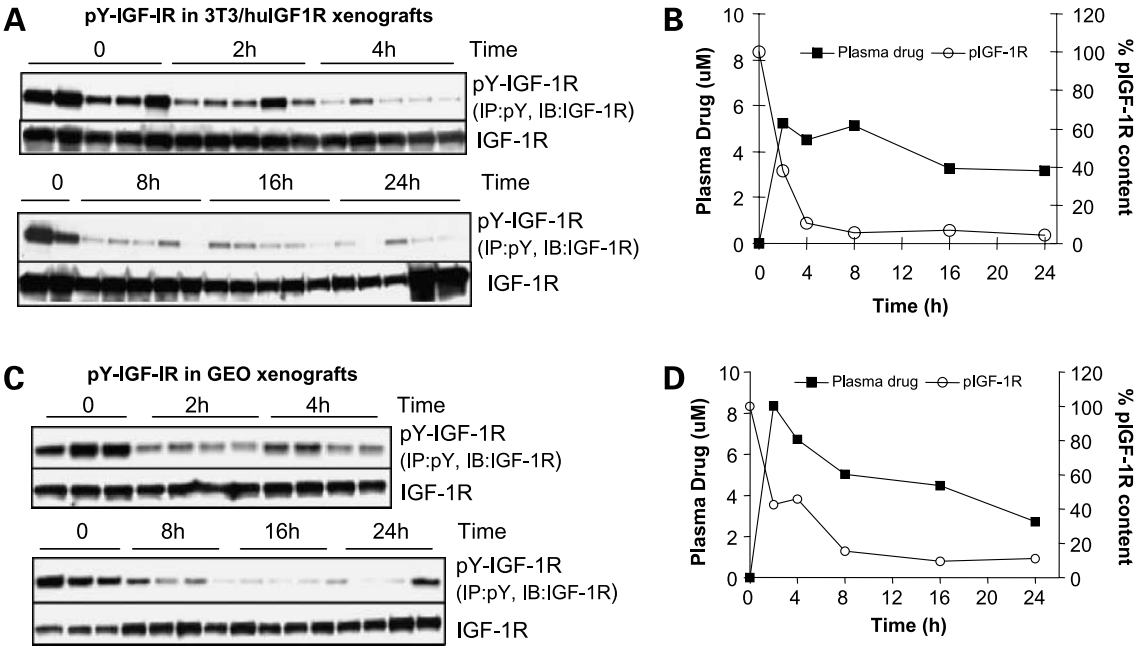

Figure 3. Pharmacokinetic/pharmacodynamic relationship of orally dosed PQIP in tumor xenograft models. **A,** effect on IGF-IR phosphotyrosine content in 3T3/huIGF1R tumor xenografts for 24 h after a single oral dose of 75 mg/kg PQIP. **B,** quantitation of the extent of inhibition of IGF-IR phosphorylation (○) in 3T3/huIGF1R tumor xenografts and the relationship with plasma levels of PQIP (■) after a single oral dose of 75 mg/kg PQIP. **C,** effect on IGF-IR phosphotyrosine content in GEO tumor xenografts for 24 h after a single oral dose of 100 mg/kg PQIP. **D,** quantitation of the extent of inhibition of IGF-IR phosphorylation (○) in GEO tumor xenografts and the relationship with plasma levels of PQIP (■) after a single oral dose of 100 mg/kg PQIP.

Published OnlineFirst August 1, 2007; DOI: 10.1158/1535-7163.MCT-07-0070

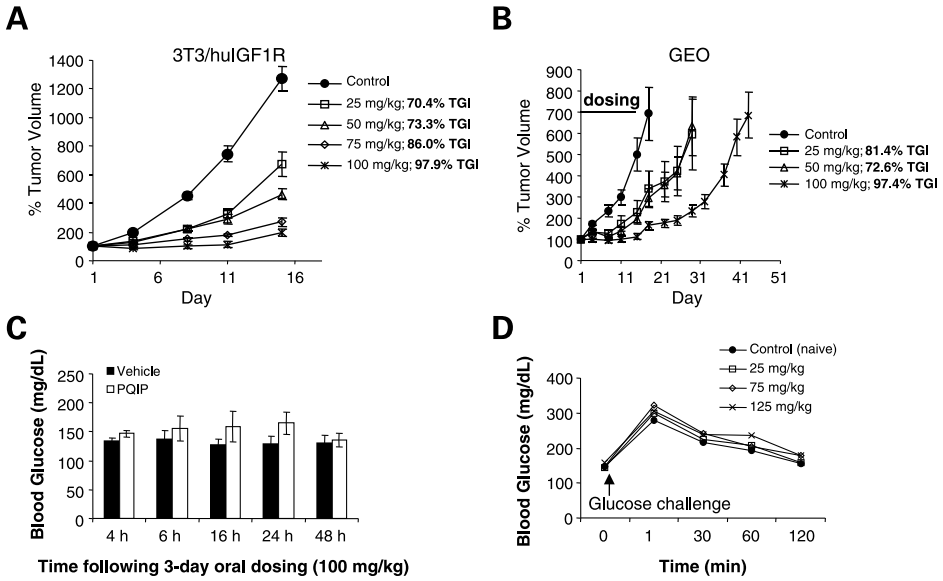

Figure 4. Antitumor activity and effect on blood glucose of orally dosed PQIP in mouse models. **A,** dose-dependent inhibition of 3T3/huIGF1R tumor xenograft growth by once daily oral dosing of PQIP for 14 d. **B,** dose-dependent inhibition of GEO tumor xenograft growth by once daily oral dosing of PQIP for 14 d, followed by outgrowth of tumors in the absence of dosing. **C,** effect on nonfasting blood glucose at indicated times in CD-1 mice after 3-d dosing of PQIP at 100 mg/kg. **D,** effect on glucose clearance in fasted CD-1 mice after 3-d dosing at 25, 75, or 125 mg/kg PQIP. Blood glucose was measured at indicated time points after the glucose challenge.

is ~10-fold less potent in blocking the insulin receptor than IGF-IR, higher concentrations of PQIP may be necessary to effectively block both IGF-IR and IR-A mediated downstream signaling contributions to GEO cell proliferation.

In vivo Efficacy of PQIP in Pharmacodynamic Models

Pharmacokinetic analysis of PQIP in mice revealed that plasma levels of PQIP (C_{max} and AUC) increased approximately linearly between oral dose levels of 5 to 200 mg/kg, and ~100% oral bioavailability of PQIP was observed when comparing the AUC to that after i.v. administration at 10 mg/kg (data not shown). In addition, plasma samples were also analyzed by high-performance liquid chromatography with UV detection at 350 nm to investigate *in vivo* metabolism. No metabolites of >10% of PQIP in plasma were detected in any samples (data not shown), suggesting that no significant contribution to *in vivo* efficacy seems to arise from metabolites in this species. These pharmacokinetic properties warranted extensive characterization of the *in vivo* effect of PQIP in mice using oral administration.

To assess the drug exposure required for inhibition of tumor IGF-IR *in vivo*, a pharmacodynamic experiment was conducted first in 3T3/huIGF1R tumors in which the relationship of inhibition of IGF-IR phosphorylation (pharmacodynamic) and drug exposure (pharmacokinetic) was evaluated after a single oral dose of 75 mg/kg (Fig. 3A and B). Greater than 95% inhibition of tumor IGF-IR phosphorylation by PQIP was achieved by 4 h and was maintained for at least 24 h at plasma drug concentrations as low as 3.85 μmol/L (Fig. 3B). In the GEO xenograft model, a single oral dose of 25 mg/kg resulted in 57% inhibition of tumor IGF-IR phosphorylation by 4 h, whereas 80% inhibition was achieved at 16 h and was maintained for at least 24 h (data not shown). In comparison, 90% inhibition of GEO tumor IGF-IR phosphorylation could be maintained for at least a 24 h period when PQIP was dosed at 100 mg/kg (Fig. 3C and D). These observations, together with the greater TGI at 75 to 100 mg/kg compared with 25 mg/kg (Fig. 4A and B), suggest that maximal antitumor efficacy requires maintenance of plasma levels sufficient to chronically suppress 90% inhibition of IGF-IR phosphorylation in tumors.

The significant phosphorylated IGF-IR levels that were detected in the GEO xenograft (Fig. 3C), but not in HT29 and H526 xenografts (data not shown), which express abundant IGF-IR, indicates that murine plasma IGF may be insufficient to activate IGF-IR in xenograft models, and likely contributes little to the activation of IGF-IR phosphorylation in the GEO xenograft. Furthermore, the IGF-IR phosphorylation detected in GEO xenograft tumors indicates that the IGF autocrine loop detected in cell culture is also operative *in vivo*.

In vivo Efficacy of PQIP in Tumor Xenograft Models

To evaluate the *in vivo* efficacy of PQIP, TGI studies were undertaken in both 3T3/huIGF1R and GEO tumor xenograft models. All of these studies were done using 25 mmol/L tartaric acid as the vehicle with once daily oral dosing of the drug for 14 consecutive days. In all of the studies, minimal effects on body weight (<10% loss) were observed, although PQIP has been found to inhibit murine IGF-IR autophosphorylation with potency similar to that observed with human IGF-IR (Supplementary Fig. S2). In the 3T3/huIGF1R model, there was significant dose-dependent TGI at all doses tested between 25 and 100 mg/kg. Daily oral dosing of 25 or 50 mg/kg resulted in 70% to 74% mean TGI over the dosing period, whereas 75 or 100 mg/kg resulted in 86% and 98% mean TGI, respectively (Fig. 4A). Antitumor efficacy was also achieved in the human GEO xenograft model when PQIP was dosed orally for 14 consecutive days (Fig. 4B). However, in the GEO model, doses of 25 and 50 mg/kg gave equivalent antitumor effects with ~70% to 80% mean TGI observed over the dosing period. Increasing the dose

Published OnlineFirst August 1, 2007; DOI: 10.1158/1535-7163.MCT-07-0070

to 100 mg/kg resulted in a mean TGI of 97% associated with a significant growth delay (24 days) after cessation of drug treatment (Fig. 4B). These TGI data, taken together with the pharmacodynamic data, suggest that 80% target inhibition is sufficient for significant antitumor effects in the GEO colon carcinoma model, whereas increasing the amount of target inhibition over 24 h further improved the antitumor efficacy.

Preclinical observations that tumors with an IGF-II/IGF-IR autocrine loop are especially sensitive to IGF-IR inhibition suggest that tumor IGF-II overexpression and/or basal IGF-IR phosphorylation may be useful biomarkers to predict clinical efficacy. IGF-II is particularly important in the context of human cancers because it is expressed in the stromal components of cancers, is present in adult humans at high circulating levels, and does not exhibit the same magnitude of age-dependent decline as IGF-I levels. Moreover, the lack of these high circulating levels of IGF-II in rodents (1) limits IGF-II/IGF-IR paracrine stimulation in tumors when using mouse models. Therefore, mouse models may underestimate the importance of the IGF pathway in human cancers, suggesting that PQIP may also be efficacious in human cancers driven by an IGF-II paracrine signaling.

Effect of PQIP on Blood Glucose in Mice

Cellular selectivity data indicate that PQIP selectively inhibits human IGF-IR relative to human and mouse IR, although mouse IR seems to be more sensitive. These data suggest that a therapeutic window would exist in the mouse, and that in humans this therapeutic window would be greater with respect to hyperglycemia. To determine whether cellular IR selectivity is predictive of a therapeutic window to allow efficacy without substantial hyperglycemia *in vivo*, PQIP was tested in nonfasted mice. Following 3 consecutive daily oral doses of vehicle or 100 mg/kg of PQIP, <30% blood glucose elevation was observed in the PQIP-treated mice (Fig. 4C). To further evaluate the effects of PQIP on glucose clearance, a glucose tolerance test was conducted in mice treated with vehicle alone or with PQIP at 25, 75, or 125 mg/kg for 3 consecutive days. Before administration of the glucose load, there was no increase in fasting blood glucose in response to PQIP. Upon administration of the glucose load, there was an ~19% AUC increase in blood glucose in the 125 mg/kg–treated animals compared with the controls. At 2 h after glucose challenge, 15% glucose elevation in mice dosed with the highest dose (125 mg/kg) of PQIP compared with the control animals was observed (Fig. 4D). Although the effect of all dose levels of PQIP on glucose clearance was slight, there was a trend toward dose dependence with lower PQIP doses showing lesser effects. These data suggest that selective IGF-IR kinase inhibitors like PQIP may provide a therapeutic window in humans for maintaining an efficacious exposure without significantly affecting blood glucose.

In summary, PQIP represents a potent and selective small-molecule kinase inhibitor of IGF-IR. The cellular selectivity for human IGF-IR relative to the insulin receptor confers a therapeutic index to inhibit IGF-IR–driven tumor growth *in vivo* without causing significant hyperglycemia. Given that IGF-IR–mediated proliferative and survival signaling is required for some human malignancies, PQIP and related IGF-IR kinase inhibitors represent promising anticancer therapeutics, particularly for tumors that depend on IGF-II autocrine or paracrine signaling. In addition, activation of the IGF-IR protects tumor cells from apoptosis induced by a variety of anticancer agents (30, 46–48), and PQIP can potentiate the efficacy of other antitumor agents, such as erlotinib (49). Hence, this class of IGF-IR inhibitors should have broad clinical utility for treatment of cancers alone or in combination with other antitumor therapies.

References

1. LeRoith D, Roberts CT, Jr. The insulin-like growth factor system and cancer. Cancer Lett 2003;195:127 – 37.
2. Ullrich A, Schlessiger J. Signal transduction by receptors tyrosine kinase activity. Cell 1990;61:203 – 12.
3. Baserga R, Peruzzi F, Reiss K. The IGF-1 receptor in cancer biology. Int J Cancer 2003;107:873 – 7.
4. Pollak MN, Schernhammer ES, Hankinson SE. Insulin-like growth factors and neoplasia. Nat Rev Cancer 2004;4:505 – 18.
5. Wang Y, Sun Y. Insulin-like growth factor receptor-1 as an anti-cancer target: blocking transformation and inducing apoptosis. Curr Cancer Drug Targets 2002;2:191 – 207.
6. Zhang H, Yee D. The therapeutic potential of agents targeting the type I insulin-like growth factor receptor. Expert Opin Investig Drugs 2004;13:1569 – 77.
7. Resnicoff M, Coppola D, Sell C, Rubin R, Ferrone S, Baserga R. Growth inhibition of human melanoma cells in nude mice by antisense strategies to type 1 insulin-like growth factor receptor. Cancer Res 1994;54:4848 – 50.
8. Chernicky CL, Yi L, Tan H, Gan SU, Ilan J. Treatment of human breast cancer cells with antisense RNA to the type I insulin-like growth factor receptor inhibits cell growth, suppresses tumourigenesis, alters the metastatic potential and prolongs survival *in vivo*. Cancer Gene Ther 2000;7:384 – 95.
9. Maloney EK, McLaughlin JL, Dagdigian NE, et al. An anti-insulin-like growth factor I receptor antibody that is a potent inhibitor of cancer cell proliferation. Cancer Res 2003;63:5073 – 83.
10. Wang Y, Hailey J, Williams D, et al. Inhibition of insulin-like growth factor-I receptor (IGF-1R) signaling and tumor cell growth by a fully human neutralizing anti-IGF-1R antibody. Mol Cancer Ther 2005;4:1214 – 21.
11. Cohen BD, Baker DA, Soderstrom C, et al. Combination therapy enhances the inhibition of tumor growth with the fully human anti-type 1 insulin-like factor receptor monoclonal antibody CP-751,871. Clin Cancer Res 2005;11:2063 – 73.
12. Goetsch L, Gonzalez A, Leger O, et al. A recombinant humanized anti-insulin-like growth factor receptor type I antibody (h7C10) enhances the antitumor activity of vinorelbine and anti-epidermal growth factor receptor therapy against human cancer xenografts. Int J Cancer 2005;113:316 – 28.
13. Prager D, Li HL, Asa S, Melmed S. Dominant negative inhibition of tumourigenesis *in vivo* by human insulin-like growth factor I receptor mutant. Proc Natl Acad Sci U S A 1994;91:2181 – 5.
14. Kalebic T, Blakesley V, Slade C, Plasschaert S, Leroith D, Helman LJ. Expression of a kinase-deficient IGF-I-R suppresses tumorigenicity of rhabdomyosarcoma cells constitutively expressing a wild type IGF-I-R. Int J Cancer 1998;76:223 – 7.
15. Scotlandi K, Avnet S, Benini S, et al. Expression of an IGF-I receptor dominant negative mutant induces apoptosis, inhibits tumourigenesis and enhances chemosensitivity in Ewing's sarcoma cells. Int J Cancer 2002;101:11 – 6.
16. Garcia-Echeverria C, Pearson MA, Marti A, et al. *In vivo* antitumor activity of NVP-AEW541—a novel, potent, and selective inhibitor of the IGF-1R kinase. Cancer Cell 2004;5:231 – 9.
17. Haluska P, Carboni JM, Loegering DA, et al. *In vitro* and *in vivo* antitumor effects of the dual insulin-like growth factor-I/insulin receptor inhibitor, BMS-554417. Cancer Res 2006;66:362 – 71.

Published OnlineFirst August 1, 2007; DOI: 10.1158/1535-7163.MCT-07-0070

18. Garcia-Echeverria C. Medicinal chemistry approaches to target the kinase activity of IGF-1R. IDrugs 2006;9:415 – 9.

19. Larsson O, Girnita A, Girnita L. Role of insulin-like growth factor I receptor signalling in cancer. Br J Cancer 2005;92:2097 – 101.

20. El-Badry OM, Helman LJ, Chatten J, et al. Insulin-like growth factor II-mediated proliferation of human neuroblastoma. J Clin Invest 1991;87: 648 – 57.

21. Quinn KA, Treston AM, Unsworth EJ, et al. Insulin-like growth factor expression in human cancer cell lines. J Biol Chem 1996;271:11477 – 83.

22. Vella V, Pandini G, Sciacca L, et al. A novel autocrine loop involving IGF-II and the insulin receptor isoform-A stimulates growth of thyroid cancer. J Clin Endocrinol Metab 2002;87:245 – 54.

23. Qing RQ, Schmitt S, Ruelicke T, Stallmach T, Schoenle EJ. Autocrine regulation of growth by insulin-like growth factor (IGF)-II mediated by type I IGF-receptor in Wilms tumor cells. Pediatr Res 1996;39:160 – 5.

24. Ma J, Pollak MN, Giovannucci E, et al. Prospective study of colorectal cancer risk in men and plasma levels of insulin-like growth factor (IGF)-I and IGF- binding protein-3. J Natl Cancer Inst 1999;91:620 – 5.

25. Chan JM, Stampfer MJ, Giovannucci E, et al. Plasma insulin-like growth factor-I and prostate cancer risk: a prospective study. Science 1998;279:563 – 6.

26. Hankinson SE, Willett WC, Colditz GA, et al. Circulating concentrations of insulin-like growth factor-I and risk of breast cancer. Lancet 1998;351:1393 – 6.

27. Yu H, Spitz MR, Mistry J, Gu J, Hong WK, Wu X. Plasma levels of insulin-like growth factor-I and lung cancer risk: a case-control analysis. J Natl Cancer Inst 1999;91:151 – 6.

28. Zhao H, Grossman HB, Spitz MR, Lerner SP, Zhang K, Wu X. Plasma levels of insulin-like growth factor-1 and binding protein-3, and their association with bladder cancer risk. J Urol 2003;169:714 – 7.

29. Parker AS, Cheville JC, Janney CA, Cerhan JR. High expression levels of insulin-like growth factor-I receptor predict poor survival among women with clear-cell renal cell carcinomas. Hum Pathol 2002;33:801 – 5.

30. Chakravarti A, Loeffler JS, Dyson NJ. Insulin-like growth factor receptor-I mediates resistance to anti-epidermal growth factor receptor therapy in primary human glioblastoma cells through continued activation of phosphoinositide 3-kinase signaling. Cancer Res 2002;62:200 – 7.

31. Zhang L, Zhou W, Velculescu VE, et al. Gene expression profiles in normal and cancer cells. Science 1997;276:1268 – 71.

32. Hassan AB, Macaulay VM. The insulin-like growth factor system as a therapeutic target in colorectal cancer. Ann Oncol 2002;13:349 – 56.

33. Chen CL, Ip SM, Cheng D, Wong LC, Ngan HY. Loss of imprinting of the IGF-II and H19 genes in epithelial ovarian cancer. Clin Cancer Res 2000;6:474 – 9.

34. Kalli KR, Falowo OI, Bale LK, Zschunke MA, Roche PC, Conover CA. Functional insulin receptors on human epithelial ovarian carcinoma cells: implications for IGF-II mitogenic signaling. Endocrinology 2002;143: 3259 – 67.

35. Kondo M, Suzuki H, Ueda R, et al. Frequent loss of imprinting of the H19 gene is often associated with its overexpression in human lung cancers. Oncogene 1995;10:1193 – 8.

36. Wang Z, Ruan YB, Guan Y, Liu SH. Expression of IGF-II in early experimental hepatocellular carcinomas and its significance in early diagnosis. World J Gastroenterol 2003;9:267 – 70.

37. Cui H, Cruz-Correa M, Giardiello FM, et al. Loss of IGF2 imprinting: a potential marker of colorectal cancer risk. Science 2003;299:1753 – 5.

38. Arnold LD, Cesario C, Coate H, et al. 6,6-Bicyclic ring substituted heterobicyclic protein kinase inhibitors. PCT International Patent Application WO 2005/097800A1.

39. Garton AJ, Crew AP, Franklin M, et al. OSI-930: a novel selective inhibitor of kit and kinase insert domain receptor tyrosine kinases with antitumor activity in mouse xenograft models. Cancer Res 2006;66: 1015 – 24.

40. Ji QS, Winnier GE, Niswender KD et al. Essential role of the tyrosine kinase substrate phospholipase C-γ1 in mammalian growth and development. Proc Natl Acad Sci U S A 1997;94:2999 – 3003.

41. Haluzik M, Yakar S, Gavrilova O, Setser J, Boisclair Y, LeRoith D. Insulin resistance in the liver-specific IGF-1 gene-deleted mouse is abrogated by deletion of the acid-labile subunit of the IGF-binding protein-3 complex: relative roles of growth hormone and IGF-1 in insulin resistance. Diabetes 2003;52:2483 – 9.

42. Duronio V. Insulin receptor is phosphorylated in response to treatment of HepG2 cells with insulin-like growth factor I. Biochem J 1990;270:27 – 32.

43. Hurbin A, Dubrez L, Coll JL, Favrot MC. Inhibition of apoptosis by amphiregulin via an insulin-like growth factor-1 receptor-dependent pathway in non-small cell lung cancer cell lines. J Biol Chem 2002;277: 49127 – 33.

44. Kaufmann SH, Desnoyers S, Ottaviano Y, Davidson NE, Poirier GG. Specific proteolytic cleavage of poly(ADP-ribose) polymerase: an early marker of chemotherapy-induced apoptosis. Cancer Res 1993;53: 3976 – 85.

45. Hailey J, Maxwell E, Koukouras K, Bishop WR, Pachter JA, Wang Y. Neutralizing anti-insulin-like growth factor receptor 1 antibodies inhibit receptor function and induce receptor degradation in tumor cells. Mol Cancer Ther 2002;1:1349 – 53.

46. Lu Y, Zi X, Pollak M. Molecular mechanisms underlying IGF-I-induced attenuation of the growth-inhibitory activity of trastuzumab (Herceptin) on SKBR3 breast cancer cells. Int J Cancer 2004;108:334 – 41.

47. Beech DJ, Perer E, Helms J, Gratzer A, Deng N. Insulin-like growth factor-I receptor activation blocks doxorubicin cytotoxicity in sarcoma cells. Oncol Rep 2003;10:181 – 4.

48. Peretz S, Jensen R, Baserga R, Glazer PM. ATM-dependent expression of the insulin-like growth factor-I receptor in a pathway regulating radiation response. Proc Natl Acad Sci U S A 2001;98: 1676 – 81.

49. Ji QS, Mak G, O'Connor M, et al. A novel IGF-1R small molecule inhibitor potentiates erlotinib activity in NSCLC cell lines *in vitro* and *in vivo* [abstract]. Proc Supplement AACR 2006;97:74.

AACR American Association for Cancer Research

Molecular Cancer Therapeutics

A novel, potent, and selective insulin-like growth factor-I receptor kinase inhibitor blocks insulin-like growth factor-I receptor signaling *in vitro* and inhibits insulin-like growth factor-I receptor–dependent tumor growth *in vivo*

Qun-sheng Ji, Mark J. Mulvihill, Maryland Rosenfeld-Franklin, et al.

Mol Cancer Ther 2007;6:2158-2167. Published OnlineFirst August 1, 2007.